Travelling waves in chains of pulse-coupled integrate-and-fire oscillators with distributed delays

P. C. Bressloff and S. Coombes

Nonlinear and Complex Systems Group, Department of Mathematical Sciences, Loughborough University, Loughborough, Leicestershire, LE11 3TU, U. K.

Abstract

We analyse travelling waves in a chain of pulse-coupled integrate-and-fire oscillators with nearest-neighbour coupling and delayed interactions. This is achieved by approximating the equations for phase-locking in terms of a singularly perturbed two-point (continuum) boundary value problem. The latter has a solution provided that a self-consistent value for the collective frequency of oscillations can be found. We investigate how the qualitative behaviour of travelling waves depends on the distribution of natural frequencies across the chain and the form of delayed interactions. A linear stability analysis of phase-locked solutions is carried out in terms of perturbations of the firing times of the oscillators. It is shown how travelling waves destabilize when the detuning between oscillators or the strength of the coupling becomes too large.

1. Introduction

One of the oldest problems in dynamics is the behaviour of coupled nonlinear oscillators, dating back to Huygen's observations of mutual synchronization of pendulum clocks in the seventeenth century. In more recent times there has been a renewed interest in coupled oscillators stimulated by a diverse range of applications including biological rhythms [1, 2], chemical oscillators [3], Josephson junction arrays [4, 5] and laser arrays [6, 7]. An important theoretical technique for analysing such systems is to work in the weak coupling regime where invariant manifold theory [8] and averaging theory [9] can be used to reduce the dynamics to a set of phase equations in which the relative phase between oscillators is the relevant dynamical variable (see, for example, [10, 11, 12]). This phase reduction method has been applied to a number of important physical and biological systems. For example, an averaged phase equation has been used to describe a linear series array of overdamped, resistively loaded Josephson junctions [13], and this has elucidated the integrable structure of the system [14]. In the biological context, phase equations have been used to study travelling waves in chains of weakly coupled oscillators that model processes such as the generation and control of rhythmic activity in central pattern generators (CPGs) underlying locomotion [15, 16] and peristalsis in vascular and intestinal

smooth muscle [11]. Related phase models (see eg. [17]) have been motivated by the observation that synchronization and waves of excitation can occur during sensory processing in the cortex [18, 19].

One of the characteristic features of a variety of biological oscillators is that they communicate with each other by firing sudden pulse-like discharges. Modelling the detailed shape of these pulses requires a system of smooth differential equations with several degrees of freedom for each oscillator. One well known example is the Hodgkin-Huxley model of excitable nerve tissue that describes the generation of an action potential due to the activation-deactivation of a number of voltage-dependent ionic gates [20]. Analysing a network of Hodgkin-Huxley neurons is a difficult task due to the complexity of the single-neuron model. This motivates the application of the phase reduction method (for weak coupling) to reduce the network dynamics to a system of phase equations with the phase interaction function constructed from the single neuron dynamics. The latter has been carried out explicitly for the Hodgkin-Huxley model [21]. An alternative approach is to neglect details concerning the shape of a pulse by considering an *integrate-and-fire* model [22]. The integrate-and-fire model has been used to study flashing fireflies [23], cardiac pacemaker cells [24], and biological neural networks [25, 26, 27, 28, 29, 30]. Mutual synchronization of integrate-and-fire oscillators has also recently sparked interest within the physics community due to certain parallels with stick-slip models and self-organized criticality [31].

Although considerable simplification is achieved by working with integrate-and-fire oscillators, the mathematical analysis is still a challenging problem since the state of the system changes discontinuously at certain discrete time (threshold crossing) events so that a complete description in terms of smooth ordinary differential equations is no longer possible. Significant progress can be made, however, once it is realised that in the case of phase-locked solutions such as synchronous states and travelling waves, the system can be described in terms of a set of phase equations involving the relative shifts in the firing times of the oscillators (with the collective frequency of the oscillators determined self-consistently). These steady-state phase equations have the same formal structure as those obtained using phase reduction methods, with the important additional feature that they are also valid in the strong coupling regime. Thus various analytical techniques developed for studying phase-locking in weakly coupled oscillators may be extended to the case of integrate-and-fire oscillators with arbitrary coupling.

In this paper we present a detailed analysis of phase-locking in networks of integrate-and-fire oscillators. For concreteness, we consider the particular problem of travelling waves along chains of integrate-and-fire oscillators with local, delayed interactions. A corresponding analysis of rings of pulse-coupled oscillators based on group theoretic methods will be presented elsewhere [32, 33]. We begin in section 2 by reviewing relevant results concerning phase-locking and travelling waves in chains of weakly coupled limit cycle oscillators. We then derive conditions for phase-locking in a chain of integrate-and-fire oscillators for arbitrary coupling strength (section 3). We also derive conditions for the linear stability of phase-locked solutions by considering small perturbations of

the firing times. In section 4 we extend a continuum approximation method introduced by Kopell and Ermentrout [34] to analyse travelling waves in long chains of integrate-and-fire oscillators. Finally, in section 5 we study through numerical examples how various instabilities arise with changes in the degree of anisotropy, the coupling strength and the distribution of external inputs.

Note that one possible application of our work is to the study of central pattern generators for locomotion. The generation and control of rhythmic activity results from a combination of synaptic interactions, intrinsic membrane properties and network connectivity. Guided by the study of small networks in the spinal cord of the lamprey or Xenopus tadpole and other experimentally accessible systems the fundamental properies of neurons that contribute to rhythm generation are being uncovered. It is likely that each oscillator is actually a local subnetwork of neurons rather than a single endogenous pacemaker cell. Since the precise details underlying such oscillators are still unknown the aim of our mathematical analysis is not to provide an accurate model of CPGs but rather to gain insight into the general forms of behaviour that chains of pulse-coupled oscillators can exhibit.

2. Phase-locking in chains of weakly coupled limit cycle oscillators

In an important series of papers, Ermentrout and Kopell carried out a detailed study of the dynamics of a chain of weakly coupled limit cycle oscillators [11, 35, 34]. A particular version of the system of equations that they considered is (for anisotropic, nearest neighbour coupling)

$$\dot{X}_n = F(X_n) + \epsilon \left[G^+(X_{n+1}, X_n) + G^-(X_{n-1}, X_n) \right] \tag{2.1}$$

where $X_n \in \mathbb{R}^k$, $n = 1, ...N+1$, $F : \mathbb{R}^k \to \mathbb{R}^k$, $G^{\pm} : \mathbb{R}^{2k} \to \mathbb{R}^k$ and the boundary conditions are $G^+(X_{N+2}, X_{N+1}) \equiv 0 \equiv G^-(X_0, X_1)$. In the absence of any coupling ($\epsilon = 0$), the nth oscillator is assumed to have a stable limit cycle with frequency ω_n. In the case of weak coupling, $\epsilon \ll 1$, it was proven using invariant manifold theory that there exists an asymptotically stable invariant torus of dimension $N+1$. Moreover, phase variables $\theta_n \in \mathbb{R} \setminus \mathbb{Z}$, $n = 1, ..., N+1$, may be chosen so that the dynamics on the torus can be expressed in the form [11]

$$\begin{aligned} \dot{\theta}_1 &= \omega_1 + \epsilon h^+(\theta_1, \theta_2, \epsilon) \\ \dot{\theta}_n &= \omega_n + \epsilon \left[h^+(\theta_n, \theta_{n+1}, \epsilon) + h^-(\theta_n, \theta_{n-1}, \epsilon) \right] \\ \dot{\theta}_{N+1} &= \omega_{N+1} + \epsilon h^-(\theta_{N+1}, \theta_N, \epsilon) \end{aligned} \tag{2.2}$$

where $h^{\pm}$ is a periodic function of its θ arguments that depends on the nature of the coupling and on the dynamics in a neighbourhood of a limit cycle. If $\omega_n = \omega_1 + \mathcal{O}(\epsilon)$ then averaging theory [9] implies that

$$\begin{aligned} \dot{\theta}_1 &= \omega_1 + \epsilon H^+(\theta_2 - \theta_1) + \mathcal{O}(\epsilon^2) \\ \dot{\theta}_n &= \omega_n + \epsilon \left[H^+(\theta_{n+1} - \theta_n) + H^-(\theta_{n-1} - \theta_n) \right] + \mathcal{O}(\epsilon^2) \\ \dot{\theta}_{N+1} &= \omega_{N+1} + \epsilon H^-(\theta_N - \theta_{N+1}) + \mathcal{O}(\epsilon^2) \end{aligned} \tag{2.3}$$

with

$$H^{\pm}(\phi) = \int_0^1 h^{\pm}(\theta, \theta + \phi, \epsilon) d\theta \tag{2.4}$$

A basic issue concerning the dynamics of a chain of coupled oscillators is the conditions under which phase-locking can occur, by which we mean a stable periodic solution to equation (2.3) and hence to equation (2.1). Such a solution takes the form $\theta_n(t) = \Omega t + \zeta_n$, where Ω is the collective frequency of oscillations and the ζ_n's are constant. Of particular interest from the viewpoint of biological systems are travelling wave solutions for which the phase ζ_n varies monotonically along the chain (see eg. [15]). For sufficiently small ϵ, phase-locked solutions of equation (2.3) correspond to fixed points of an associated system of equations for the phase-differences $\phi_n = \theta_{n+1} - \theta_n$, $n = 1, ..., N$:

$$\dot{\phi}_n = \Delta_n + H^+(\phi_{n+1}) - H^+(\phi_n) + H^-(-\phi_n) - H^-(-\phi_{n-1}) \tag{2.5}$$

with boundary conditions

$$H^-(-\phi_0) \equiv 0 \equiv H^+(\phi_{N+1}) \tag{2.6}$$

where $\epsilon\Delta_n = \omega_{n+1} - \omega_n$ and the time t has been rescaled according to $t \to \epsilon t$. Note that fixed points of equation (2.5) are independent of the collective frequency Ω; the latter is determined from the equation

$$\Omega = \omega_1 + \epsilon H^+(\phi_1) + \mathcal{O}(\epsilon^2) \tag{2.7}$$

One finds that there are at least two different mechanisms that can generate travelling wave solutions. The first is based on the presence of a gradient of frequencies along the chain, that is, Δ_n has the same sign for all n, with the wave propagating from the high frequency region to the low frequency region. This can be established explicitly in the case of an isotropic, odd interaction function, $H^{\pm}(\phi) = H(\phi) = -H(-\phi)$. Equation (2.5) then simplifies according to

$$\dot{\phi}_n = \Delta_n + H(\phi_{n+1}) + H(\phi_{n-1}) - 2H(\phi_n) \tag{2.8}$$

so that fixed point solutions $\Phi = (\phi_1, ..., \phi_N)$ satisfy the matrix equation

$$\mathbf{H}(\Phi) = -\mathbf{A}^{-1}\mathbf{D} \tag{2.9}$$

where $\mathbf{H}(\Phi) = (H(\phi_1), ..., H(\phi_n))^{\top}$, $\mathbf{D} = (\Delta_1, ..., \Delta_N)^{\top}$, and $\mathbf{A}$ is a tridiagonal matrix with components $A_{ii} = -2$, $A_{i,i+1} = A_{i+1,i} = 1$. For the sake of illustration suppose that $H(\phi) = \sin 2\pi\phi$. Then a solution Φ will exist if every component of $\mathbf{A}^{-1}\mathbf{D}$ lies between ± 1. Let $a_0 = \max_n\{|\left(\mathbf{A}^{-1}\mathbf{D}\right)_n|\}$. If $a_0 < 1$ then for each $n = 1, ..., N$ there are two distinct solutions $\phi_n^{\pm}$ in the interval $[0, 1]$ with $H'(\phi_n^-) > 0$ and $H'(\phi_n^+) < 0$. In other words, there are 2^N phase-locked solutions. Linearizing equation (2.8) about a phase-locked solution Φ and exploiting the structure of the matrix $\mathbf{A}$, it can be proven that only the

solution $\Phi^- = (\phi_1^-, ..., \phi_N^-)$ is stable. Assuming that the frequency gradient is monotonic, this solution corresponds to a stable travelling wave. When the gradient becomes too steep to allow phase-locking (i.e. $a_0 > 1$), two or more pools of oscillators (frequency plateaus) tend to form that oscillate at different frequencies [11].

Waves induced by frequency differences are important in peristalsis [36, 11] and are also known to exist in certain central pattern generators (CPGs) for swimming including the leech [37] and the Xenopus tadpole [38]. However, there is no evidence for frequency gradients in the lamprey CPG [15]. Moreover, in contrast to the waves observed in the lamprey CPG, waves produced by a frequency gradient do not have a constant speed or, equivalently, constant phase lags along the chain. Constant speed waves in a chain of identical oscillators can be generated by an alternative mechanism based on properties of the coupling. This can be understood by considering a chain of identical oscillators with one-way coupling. Setting $H^- = 0$ and $\Delta_n = 0$ in equation (2.5) shows that if there exists a non-zero value $\overline{\phi}$ at which $H^+(\overline{\phi}) = 0$, $H^{+\prime}(\overline{\phi}) > 0$ then there exists a stable travelling wave solution with constant phase lag, $\phi_n = \overline{\phi}$ for all n. An interaction function having the above so-called *edge property* occurs for almost all kinds of coupling including chemical synapses. One important exception is that of electrical synapses (gap junctions) where the coupling is diffusive so that $G^{\pm}(U, U) = 0$ in equation (2.1) and hence $H^{\pm}(0) = 0$. If the coupling is in both directions, as in the lamprey CPG, then the analysis is considerably more involved. Nevertheless, it can be shown that for non-diffusive, anisotropic coupling, $H^+ \neq H^-$, $H^{\pm}(0) \neq 0$, and sufficiently long chains of identical oscillators, there exists stable travelling waves with constant phase lags (except in a small boundary layer). The method of proof involves a continuum limit analysis in which solutions of equation (2.5) are shown to converge to solutions of a class of nonlinear, singularly perturbed, two-point boundary value problems [35, 34].

An important question concerning the dynamics of weakly coupled oscillators is how large the coupling strength ϵ is permitted to be without the loss of the invariant torus. If the rate of attraction to the limit cycle is sufficiently strong an equation of the form (2.2) also holds in the strong coupling regime. One then has a phase model whose interaction functions no longer depend on phase differences (since averaging theory is no longer appropriate). Such a model can exhibit more complex behaviour than the averaged model. In particular, for sufficiently large interactions, the coupling can act to stop all oscillations leading to so-called *oscillator death*. This has been studied in some detail for several models of excitable cells in which the function $h^{\pm}$ naturally takes the product form [39, 40]

$$h(\theta_n, \theta_m, \epsilon) = \epsilon R(\theta_n) P(\theta_m) \tag{2.10}$$

where $P(\theta)$ is a positive pulse-like function (associated with conductances) and $R(\theta)$ is analogous to the phase-response curve for a forced oscillator [2].

In this paper, we shall consider another class of models for coupled excitable cells that is based on the integrate-and-fire model of neural oscillators. Such a

model, which may be regarded as a reduction of the Hodgkin-Huxley model [41], preserves the pulse-like nature of neural interactions without being concerned about the particular details of the shape of action potentials. It will allow us to incorporate various details concerning neural interactions, such as axonal transmission delays and synaptic processing, in a relatively straightforward manner. As we shall establish in section 3, one of the interesting features of integrate-and-fire chains is that the conditions for phase-locking are formally identical to those derived from equation (2.3) except that the former hold for all values of the coupling strength ϵ rather than just in the weak coupling limit. Thus one can extend the continuum approximation method of Kopell and Ermentrout [34] to analyse travelling waves in chains of integrate-and-fire oscillators, with the important additional feature that the analysis holds for arbitrary values of the coupling strength ϵ (see section 4).

3. Phase-locking in chains of integrate-and-fire oscillators

3.1. The model

Consider a chain of $N+1$ integrate-and-fire oscillators labelled $n = 1, ..., N+1$. Let $U_n(t)$ denote the state of the nth oscillator at time t. Suppose that the variables $U_n(t)$ satisfy the set of coupled equations

$$\dot{U}_n(t) = -\frac{U_n(t)}{\tau_s} + I_n + \epsilon \sum_{\langle m,n \rangle} \widehat{E}_m(t) \tag{3.1}$$

for $0 < U_n < 1$ where $\langle ., n \rangle$ denotes summation over nearest neighbours of n. Here τ_s represents a membrane time constant and ϵ corresponds to a conductance (in appropriate units). For convenience, we fix the units of time by setting $\tau_s = 1$. Typical values of the membrane time constant are $5 - 20$ msec. Equation (3.1) is supplemented by the condition that the oscillator fires a single pulse or spike whenever $U_n = 1$ and that the state is immediately reset to $U_n = 0$. In equation (3.1), I_n denotes a fixed external input and $\widehat{E}_n$, $n = 1, ..., N+1$, represents the input from the nth oscillator. We shall assume that $I_n > 1$ so that in the absence of any coupling ($\epsilon = 0$) each oscillator fires at a rate $1/\overline{T}_n$ with $\overline{T}_n = \ln [I_n/(I_n - 1)]$. The inputs take the form

$$\widehat{E}_m(t) = \int_0^\infty \rho(\tau) E_m(t - \tau) d\tau \tag{3.2}$$

for $m = 1, ..., N+1$, where $E_m(t)$ is the sequence of spikes transmitted from the mth oscillator at time t and $\rho(\tau)$ specifies a distribution of delayed connections. Neglecting the shape of an individual pulse, each spike train can be represented as a sequence of Dirac delta-functions

$$E_n(t) = \sum_{j=-\infty}^{\infty} \delta(t - T_j^n) \tag{3.3}$$

where T_j^n is the jth firing-time of the nth oscillator, that is, $U_n(T_j^n) = 1$.

We decompose $\rho(\tau)$ as $\rho(\tau) = \rho_e(\tau) - \rho_i(\tau)$ where $\rho_{e,i}(\tau)$ represent distributions of excitatory (e) and inhibitory (i) connections between neighbouring oscillators with $\rho_{e,i}(\tau) \geq 0$ for all τ and $\int_0^\infty \rho_{e,i}(\tau)d\tau = W_{e,i} < \infty$. In neural circuits underlying locomotion [38] and cortical microcircuits [42], there is a mixture of excitation and inhibition mediated through synaptic interactions. In fact both inhibitory and excitatory post synaptic potentials (PSPs) have some finite rise and fall time. Moreover, the former are often generated by inhibitory interneurons leading to another form of delay in the interaction process. Motivated by such architectures we take

$$\rho_e(\tau) = \tau\alpha^2 \exp(-\alpha\tau)\Theta(\tau), \quad \rho_i(\tau) = \rho_e(\tau - \tau_d) \tag{3.4}$$

where $\Theta(x) = 1$ if $x \geq 0$ and $\Theta(x) = 0$ if $x < 0$. In this case the inhibitory pathway is delayed with respect to the excitatory one and both forms of PSP are assumed to be identical with $W_{e,i} = 1$. An analogous construction is considered by Ritz *et al* [43]. For the moment we shall also assume that the connections between oscillators are isotropic. In section 4 we shall relax this assumption to allow for anisotropy. This requires the introduction of a pair of distributions for right-directed delayed interactions, $\rho^+(\tau)$ and similarly for left-directed connections $\rho^-(\tau)$.

3.2. Phase-reduction and averaging in the weak coupling limit

We shall first show how in the weak coupling limit equation (3.1) with reset can be reduced to a phase equation of the form (2.2). Following van Vreeswijk *et al* [44], we introduce the phase variable $\psi_n(t)$ according to

$$(\text{mod } 1)\ \psi_n(t) + \frac{t}{\overline{T}_n} = \Psi_n(U_n(t)) \tag{3.5}$$

where

$$\Psi_n(U) = \frac{1}{\overline{T}_n}\int_0^U \frac{dx}{I_n - x} = \frac{1}{\overline{T}_n}\ln\left[\frac{I_n}{I_n - U}\right] \tag{3.6}$$

Under such a transformation equation (3.1) becomes

$$\dot{\psi}_n(t) = \epsilon R_{\overline{T}_n}(\psi_n(t) + t/\overline{T}_n)\sum_{\langle m,n\rangle}\widehat{E}_m(t) \tag{3.7}$$

with

$$R_T(\theta) = \frac{\left[1 - \mathrm{e}^{-T}\right]\mathrm{e}^{T\theta}}{T} \tag{3.8}$$

for $0 \leq \theta < 1$ and $R_T(\theta + j) = R_T(\theta)$ for all $j \in \mathbb{Z}$. In the absence of any coupling the phase variable $\psi_n(t)$ is constant in time and all oscillators fire with their natural periods $\overline{T}_n$. For weak coupling, each oscillator still approximately fires

at the unperturbed rate but now the phases slowly drift according to equation (3.7). Since the distribution $\rho(\tau)$ is normalizable with $\rho(\tau) \to 0$ as $\tau \to \infty$, we can neglect the contribution to $\widehat{E}_m(t)$ from spikes fired sufficiently far in the past. Hence, to first order in ϵ, we can take the firing-times to be $T_j^n = (j - \psi_n(t))\overline{T}_n$. Under this approximation, equations (3.2) and (3.7) lead to the following equation for the shifted phases $\theta_n(t) = \psi_n(t) + t/\overline{T}_n$:

$$\dot{\theta}_n = \frac{1}{\overline{T}_n} + \epsilon \sum_{\langle m,n \rangle} R_{\overline{T}_n}(\theta_n) P_{\overline{T}_m}(\theta_m) + \mathcal{O}(\epsilon^2) \tag{3.9}$$

where

$$P_T(\theta) = \sum_{j=0}^{\infty} \rho((\theta + j)T) \tag{3.10}$$

for $0 \leq \theta < 1$ and P_T is extended outside this range by taking it to be a periodic function of θ.

Comparison of equation (3.9) with equations (2.2) and (2.10) shows that R_T may be interpreted as the phase-response curve (PRC) of an individual integrate-and-fire oscillator and P_T is the corresponding pulse-like function that contains all details concerning the distribution of delays. As discussed in some detail by Hansel *et al* (1995), integrate-and-fire oscillators have a type I PRC, which means that an instantaneous excitatory stimulus always advances its phase ($R_T(\theta)$ is positive for all θ). On the other hand, in certain cases, limit cycle oscillators based on Hodgkin-Huxley-like models of excitable cells are of type II. That is, an excitatory impulse can either advance or retard the phase depending upon the point on the cycle at which the stimulus is applied ($R_T(\theta)$ takes on both positive and negative values over the domain $\theta \in [0, 1]$). Since equation (3.9) was derived in the weak coupling regime, we can simplify it further by assuming that $I_n = I + \mathcal{O}(\epsilon)$ and averaging over the period $\overline{T} = \ln[I/(I-1)]$. This leads to an equation of the form (2.3) with isotropic coupling,

$$\dot{\theta}_n = \omega_n + \epsilon \sum_{\langle m,n \rangle} H_{\overline{T}}(\theta_m - \theta_n) + \mathcal{O}(\epsilon^2) \tag{3.11}$$

with $\omega_n = 1/\overline{T}_n$ and

$$H_T(\phi) = \int_0^1 R_T(\theta) P_T(\theta + \phi) d\theta \tag{3.12}$$

(Note that an averaged interaction function for integrate-and-fire models was previously computed by Ermentrout [45]). We conclude that in the weak coupling regime, phase-locking can be analysed along the lines described in section 2 for the given interaction function (3.12).

A number of points are in order. First, the interaction function $H_{\overline{T}}$ in equation (3.12) depends explicitly on the natural frequency $1/\overline{T}$ of the oscillators.

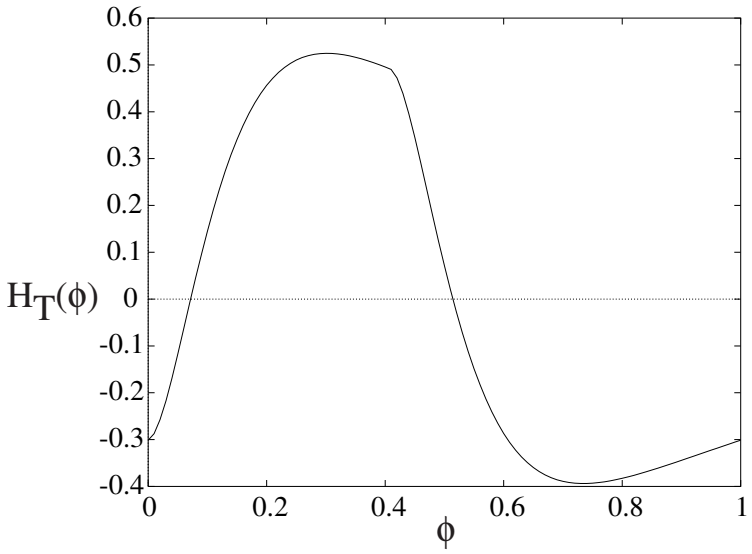


Figure 1: Isotropic interaction function $H_T(\phi)$ defined by equations (3.12) and (3.13) with $\alpha = 10$, $\tau_d = 0.6$ and $T = 1.47$.

In general, this would mean that the phase-lag induced along a chain by a travelling wave would vary with the speed of locomotion (see section 2). However, it appears that in certain vertebrates such as the lamprey, the phase-lag is approximately independent of the speed of swimming. Indeed, it is found that the wavelength of a travelling wave is comparable to the length of the animal's body. A possible mechanism for this, based on additional long-range coupling, has been considered by Ermentrout and Kopell [46]. Second, since integrate-and-fire oscillators are of type I the interaction function $H_T(\phi)$ would be positive for all ϕ in the case of purely excitatory interactions. In order to allow for the more general type II form of interaction function, we have assumed that there exists a combination of excitatory and inhibitory interactions between the integrate-and-fire oscillators, see equation (3.4). In particular, $P_T(\theta) = P_T^e(\theta) - P_T^i(\theta)$ where $P_T^{e,i} = \sum_{j=0}^{\infty} \rho_{e,i}((\theta + j)T)$. The summation over j is easily performed for $\rho_{e,i}$ satisfying equation (3.4) and gives

$$P_T^e(\theta) = \frac{\alpha^2 \mathrm{e}^{-\alpha\theta T}}{1 - \mathrm{e}^{-\alpha T}} \left[\theta T + \frac{T\mathrm{e}^{-\alpha T}}{1 - \mathrm{e}^{-\alpha T}}\right], \quad 0 \le \theta < 1, \quad P_T^i = P_T^e(\theta - \tau_d/T) \tag{3.13}$$

As before, these functions are extended outside their ranges by taking them to be periodic functions of θ. For an appropriate combination of excitatory and inhibitory connections it is possible for the effective interaction function of an integrate-and-fire oscillator to be approximately sinusoidal (see figure 1).

3.3. Phase-locked solutions for arbitrary coupling

It is possible to study phase-locked solutions of equation (3.1) without the assumption of weak coupling, as we shall now demonstrate. Suppose that every oscillator fires with the same fixed period T, which is to be determined self-consistently. The state of each oscillator can then be characterized by a constant phase $\theta_n \in \mathbb{R} \setminus \mathbb{Z}$, and the firing times of the nth oscillator become $T_j^n = (j - \theta_n)T$. Following Bressloff *et al* [32], we integrate equation (3.1) over the interval $t \in (-T\theta_n, T - T\theta_n)$ and incorporate the reset condition by setting $U_n(-\theta_n T) = 0$ and $U_n(T - \theta_n T) = 1$. This leads to the result

$$1 = (1 - \mathrm{e}^{-T})I_n + \epsilon \mathrm{e}^{-T} \sum_{\langle m,n \rangle} \int_{-\theta_n T}^{T-\theta_n T} \left[\int_0^\infty \rho(\tau) E_m(t - \tau) d\tau \right] \mathrm{e}^t dt$$

On using equation (3.3), this becomes

$$(1 - \mathrm{e}^{-T})^{-1} = I_n + \epsilon \sum_{\langle m,n \rangle} K_T(\theta_m - \theta_n), \quad n = 1, ..., N + 1 \tag{3.14}$$

where

$$K_T(\theta) = K_T^e(\theta) - K_T^i(\theta), \quad K_T^{e,i}(\theta) = (\mathrm{e}^T - 1)^{-1} \int_0^T \mathrm{e}^t P_T^{e,i}(t/T + \theta) dt \tag{3.15}$$

Note that $K_T(\theta + 1) = K_T(\theta)$.

Comparison of equation (3.14) with the corresponding set of conditions for phase-locked solutions, $\dot{\theta}_n = \Omega$, of equation (3.11) shows that they are formally identical, with K_T playing the role of the phase interaction function H_T and $\omega_n \to I_n = (1 - \mathrm{e}^{-T_n})^{-1}$, $\Omega \to (1 - \mathrm{e}^{-T})^{-1}$. Indeed, equations (3.8), (3.12) and (3.15) show that

$$K_T(\phi) = \chi H_T(\phi), \quad \chi = \frac{T^2 \mathrm{e}^{-T}}{(1 - \mathrm{e}^{-T})^2} \tag{3.16}$$

It follows that one can extend the analysis of Kopell and Ermentrout [35, 34] to construct a singularly perturbed two-point boundary value problem to investigate the existence of travelling waves in a long chain of integrate-and-fire oscillators with arbitrary coupling (see section 4). However, a number of important differences between the two models needs to be highlighted. First, equation (3.14) is exact whereas equation (3.11) is only valid to $\mathcal{O}(\epsilon)$ since it is derived under the assumption of weak coupling. Second, the collective frequency of oscillations must be determined self-consistently in equation (3.14). A third important difference between equations (3.11) and (3.14) is that although the equations for phase locking in the two models are formally the same, the underlying dynamical systems are distinct thus leading to differences in their stability properties. Note in particular that the phase-reduced model (3.11) is a finite-dimensional dynamical system whereas the integrate-and-fire model (3.1) is an infinite-dimensional one due to the presence of delays.

The linear stability of a phase-locked solution $\Phi = (\phi_1, \phi_2, ..., \phi_n)$, $\phi_n = \theta_{n+1} - \theta_n$, of equation (3.1) can be determined by considering small perturbations of the phase-locked firing patterns $T_j^n = (j - \theta_n)T$ of the form $T_j^n \to T_j^n + \delta_j^n$. This method was previously used by van Vreeswijk [47] to study globally coupled integrate-and-fire networks and was extended to more general network architectures by Bressloff and Coombes [33]. Solving equation (3.1) and the reset condition leads to an implicit map for the firing times that can be linearized to give

$$\begin{aligned}[I_n - 1 + \epsilon A_n(\Phi, T)](\delta_{k+1}^n - \delta_k^n) &+ \epsilon B_n(\Phi, T)\delta_k^n \\ &= \epsilon \sum_{\langle m,n \rangle} \sum_{j=F_k^{nm}}^{\infty} G_{nm}^j(\Phi, T)\delta_{k-j}^m \quad (3.17)\end{aligned}$$

where

$$\begin{aligned}A_n(\Phi, T) &= \sum_{\langle m,n \rangle} P_T(\theta_m - \theta_n) \\ B_n(\Phi, T) &= \frac{1 - \mathrm{e}^{-T}}{T} \sum_{\langle m,n \rangle} K_T'(\theta_m - \theta_n) \quad (3.18)\end{aligned}$$

$$G_{nm}^j(\Phi, T) = \mathrm{e}^{-T} \int_0^T \mathrm{e}^t \rho'(t + (j + \phi_m - \phi_n)T)\Theta(t + (j + \phi_m - \phi_n)T)dt \quad (3.19)$$

and $F_k^{nm} = -1$ if $T_n^{k+1} > T_m^{k+1}$ whereas $F_k^{nm} = 0$ if $T_n^{k+1} < T_m^{k+1}$. The lower limit F_k^{nm} is necessary to ensure that equation (3.17) is a *retarded* infinite-order difference equation. For small perturbations we may write $\delta_k^n = \mathrm{e}^{k\lambda}\delta_n$. Substitution into equation (3.17) yields

$$\begin{aligned}\left[(\mathrm{e}^\lambda - 1)(I_n - 1 + \epsilon A_n(\Phi, T)) \right. &+ \left. \epsilon B_n(\Phi, T)\right] \delta_n \\ &= \epsilon \sum_{\langle m,n \rangle} \widetilde{G}_{nm}(\lambda, \Phi, T)\Lambda_{nm}(\lambda)\delta_m \quad (3.20)\end{aligned}$$

where

$$\widetilde{G}_{nm}(\lambda, \Phi, T) = \sum_{k=0}^{\infty} G_{nm}^k(\Phi, T)\mathrm{e}^{-k\lambda} \quad (3.21)$$

and $\Lambda_{nm}(\lambda) = \mathrm{e}^\lambda$ if $\phi_n < \phi_m$, $\Lambda_{nm}(\lambda) = 1$ if $\phi_n > \phi_m$ on $\mathbb{R} \setminus \mathbb{Z}$. Note that since $\sum_{\langle m,n \rangle} \widetilde{G}_{nm}(0, \Phi, T) = B_n(\Phi, T)$, one solution to (3.20) is given by $\lambda = 0$ with $\delta_n = \delta$ for all n, reflecting invariance under uniform phase-shifts.

Certain care has to be taken concerning the discrete transform (3.21). Suppose that $G_{nm}^k(\Phi, T) \to \mathrm{e}^{-ks_0}$ as $k \to \infty$ for some $s_0 > 0$. Then the series on the right-hand side of equation (3.21) is only convergent for Re $\lambda > -s_0$. Imposing the latter condition on allowed solutions of equation (3.20) would correspond to excluding perturbations $\delta_k^n = \mathrm{e}^{k\lambda}\delta_n$ that blow up too quickly as $k \to -\infty$.

We shall take an alternative approach by analytically continuing $\widetilde{G}(\lambda, \Phi, T)$ into the region Re $\lambda < -s_0$. This will generate an infinite set of poles in the left-hand complex λ-plane, but these will not be important in terms of determining whether or not a phase-locked solution is stable. As a simple example, suppose that $\rho(\tau) = \alpha^2 \tau \mathrm{e}^{-\alpha\tau}$. Then $G^k_{nm}(0, T) = G_k(T)$ for all n, m where

$$G_k(T) = F_0(T)\mathrm{e}^{-k\alpha T} - kF_1(T)\mathrm{e}^{-k\alpha T} \tag{3.22}$$

$$F_0(T) = \frac{\alpha^2 \mathrm{e}^{-T}}{(1-\alpha)^2}\left[(1 - \alpha T + \alpha^2 T)\mathrm{e}^{(1-\alpha)T} - 1\right] \tag{3.23}$$

$$F_1(T) = \frac{T\alpha^3 \mathrm{e}^{-T}}{1-\alpha}\left[\mathrm{e}^{(1-\alpha)T} - 1\right] \tag{3.24}$$

so that, after summing the resulting geometric series in equation (3.21),

$$\widetilde{G}(\lambda, 0, T) = \frac{F_0(T)}{1 - \mathrm{e}^{-\alpha T - \lambda}} - \frac{F_1(T)\mathrm{e}^{-\alpha T - \lambda}}{(1 - \mathrm{e}^{-\alpha T - \lambda})^2} \tag{3.25}$$

It is clear from equation (3.25) that $\widetilde{G}(\lambda, 0, T)$ has poles at $\lambda = -\alpha T + 2i\pi n$, $n \in \mathbb{Z}$.

The condition for asymptotic stability of a travelling wave solution is Re $\lambda < 0$ for all eigenvalues other than the single eigenvalue $\lambda = 0$. The discrete spectrum is expected to consist of an infinite number of distinct eigenvalues, reflecting the fact that (3.20) is an *infinite*-order difference equation. Hence, establishing stability analytically is non-trivial in the general case. However, considerable simplification occurs in the weak-coupling limit. Suppose that $I_n = I + \mathcal{O}(\epsilon)$ for some fixed $I > 1$. For sufficiently small coupling, solutions to equation (3.20) in the complex λ-plane will either be in a neighbourhood of the real solution $\lambda = 0$ or in a neighbourhood of one of the poles of $\widetilde{G}(\lambda, \Phi, T)$. Since the latter have negative real parts bounded away from zero, the stability of the phase-locked solution will be determined by the eigenvalues close to the origin. Therefore, setting $\lambda = 0$ and $T = \overline{T} = \ln(I/(I-1))$ on the right-hand side of (3.20) yields the equation

$$(\mathrm{e}^{\lambda} - 1)(I-1)\delta_n = \frac{\epsilon}{I}\sum_{\langle m,n\rangle} K'_{\overline{T}}(\theta_m - \theta_n)[\delta_m - \delta_n] + \mathcal{O}(\epsilon^2) \tag{3.26}$$

Thus to $\mathcal{O}(\epsilon)$ the spectrum around $\lambda = 0$ coalesces into $N+1$ distinct points given by $\lambda_0 = 0$, $\lambda_p = \epsilon\mu_p + \mathcal{O}(\epsilon^2)$, $p = 1, ..., N$, with $0, \mu_1, ..., \mu_N$ the eigenvalues of the $N+1 \times N+1$ matrix $\widetilde{\mathcal{J}}_{mn}(\Phi) = \mathcal{J}_{mn}(\Phi) - \delta_{m,n}\sum_{\langle p,n\rangle}\mathcal{J}_{pn}(\Phi)$ with

$$\mathcal{J}_{mn}(\Phi) = \frac{1}{I(I-1)\overline{T}}\sum_{\langle p,n\rangle} K'_{\overline{T}}(\theta_p - \theta_n)\delta_{m,p} \tag{3.27}$$

The condition for stability reduces to $\mathrm{Re}(\mu_p) < 0$ for all $p = 1, ..., N$. Note that the same stability condition would have been obtained from the phase

model (3.11). This is an immediate consequence of the relationship between the interaction functions $H_T(\phi)$ and $K_T(\phi)$ (see equation (3.16)). Hence, up to a positive multiplier, $\widetilde{\mathcal{J}}_{mn}(\Phi)$ can be identified as the Jacobian of equation (3.11) linearized about a phase-locked solution Φ.

4. Continuum boundary value problem

4.1. Continuum model

In the previous section we derived conditions for phase-locked solutions of a chain of integrate-and-fire oscillators with nearest neighbour coupling, see equation (3.14). In the case of a long chain, we can consider a continuum version of these equations along analogous lines to the analysis of the weakly coupled phase model by Kopell and Ermentrout [34]. However, we now have to take into account the fact that we cannot solve for the phase differences ϕ_n independently of the collective frequency $1/T$. For our discussion to be sufficiently general, we shall allow for anisotropy between left and right-directed interactions so that there are now two interaction functions $K_T^{\pm}$. We use the $-$ symbol to denote the effect of the $(n-1)$th oscillator on the nth oscillator and $+$ to denote the effect of the $n+1$th oscillator on the nth oscillator. Equation (3.14) becomes

$$\begin{aligned}(1-\mathrm{e}^{-T})^{-1} &= I_1 + \epsilon K_T^+(\theta_2-\theta_1)\\ (1-\mathrm{e}^{-T})^{-1} &= I_n + \epsilon\left[K_T^+(\theta_{n+1}-\theta_n) + K_T^-(\theta_{n-1}-\theta_n)\right]\\ (1-\mathrm{e}^{-T})^{-1} &= I_{N+1} + \epsilon K_T^-(\theta_N-\theta_{N+1})\end{aligned} \tag{4.1}$$

Let

$$f_T(\phi) = \frac{1}{2}[K_T^+(\phi)+K_T^-(-\phi)], \quad g_T(\phi) = \frac{1}{2}[K_T^+(\phi)-K_T^-(-\phi)] \tag{4.2}$$

and set

$$\Omega(T) = \frac{1}{1-\mathrm{e}^{-T}} \tag{4.3}$$

Equation (4.1) can then be rewritten in the form (with $\phi_n = \theta_{n+1}-\theta_n$)

$$\Omega(T) = I_n + \epsilon\left[f_T(\phi_n) + f_T(\phi_{n-1}) + \frac{1}{N}\frac{g_T(\phi_n)-g_T(\phi_{n-1})}{1/N}\right] \tag{4.4}$$

with boundary conditions

$$\Omega(T) = I_1 + \epsilon\left[f_T(\phi_1)+g_T(\phi_1)\right] \tag{4.5}$$

$$\Omega(T) = I_{N+1} + \epsilon\left[f_T(\phi_N)-g_T(\phi_N)\right] \tag{4.6}$$

For large N equations (4.4)-(4.6) become

$$\Omega(T) = I(x) + \epsilon\left[2f_T(\phi) + \frac{1}{N}[g_T(\phi)]_x\right] \tag{4.7}$$

with boundary conditions

$$\Omega(T) = I(0) + \epsilon\,[f_T(\phi) + g_T(\phi)] \text{ at } x = 0 \tag{4.8}$$
$$\Omega(T) = I(1) + \epsilon\,[f_T(\phi) - g_T(\phi)] \text{ at } x = 1 \tag{4.9}$$

where $I(x)$ and $\phi(x)$ are the continuum limits of $\{I_n\}$ and $\{\phi_n\}$, and $0 \le x \le 1$.

Our method of solution proceeds as follows. First, we shall assume that T is fixed so that f_T and g_T are known functions and treat $\Omega(T)$ as an unknown. We shall then follow Kopell and Ermentrout [34] and use the method of matched asymptotic expansions to piece together an outer solution that satisfies

$$\Omega(T) = I(x) + 2\epsilon f_T(\phi) \tag{4.10}$$

and an inner solution that satisfies the boundary layer equation

$$0 = 2f_T(\phi)_X + [g_T(\phi)]_{XX} \tag{4.11}$$

where $X = N(x - x_0)$ with the boundary layer localized about x_0. Imposing certain conditions on the functions f_T and g_T, this will yield a unique solution to the given boundary value problem, and hence determine $\Omega(T)$. If we now treat T as a free variable we obtain a one-parameter family of solutions and $\Omega(T)$ becomes a known function of T. The final step is to solve equation (4.3) for T. This will generate a unique, self-consistent, phase-locked solution provided that equation (4.3) has a unique solution for T that does not violate the original hypotheses on the coupling functions f_T and g_T.

4.2. Matching procedure for fixed T

We begin by describing the matching procedure for fixed T [34]. We shall assume that for a given T there exist points ϕ_L, ϕ_R such that

$$K_T^+(\phi_R) \equiv f_T(\phi_R) + g_T(\phi_R) = 0, K_T^-(-\phi_L) \equiv f_T(\phi_L) - g_T(\phi_L) = 0 \tag{4.12}$$

(For ease of notation we do not make explicit the fact that ϕ_L and ϕ_R themselves depend on T). Suppose that there is not a boundary layer at $x = 0$. Then the term $[g_T(\phi)]_x$ in equation (4.7) remains $O(1)$ as $x \to 0$. Hence, $\Omega(T) = I(0) + 2\epsilon f_T(\phi) + O(1/N)$. Subtracting this from the boundary condition (4.8) at $x = 0$ gives $0 = \epsilon[f_T(\phi(0)) - g_T(\phi(0))] + O(1/N)$, which implies that $K_T^-(-\phi(0)) = 0$, that is, $\phi(0) = \phi_L$. It follows from equation (4.8) that $\Omega(T) = \Omega_L(T)$ where

$$\Omega_L(T) = I(0) + 2\epsilon f_T(\phi_L) \tag{4.13}$$

A similar argument shows that if there does not exist a boundary layer at $x = 1$ then $\phi(1) = \phi_R$ and $\Omega(T) = \Omega_R(T)$ where

$$\Omega_R(T) = I(1) + 2\epsilon f_T(\phi_R) \tag{4.14}$$

In each of these two cases, the constant $\Omega(T)$ is determined in terms of the zeros of the interaction functions $K_T^{\pm}$. As we shall illustrate later, it is also possible

for boundary layers to occur at both ends, in which case the specification of $\Omega(T)$ is slightly more involved.

Now consider a boundary layer near $x = 1$ so that $X = N(x-1)$ with $X = 0$ at $x = 1$ and $X < 0$ for $0 < x < 1$. Integrating equation (4.11) yields

$$\frac{d\phi}{dX} = \frac{A - 2f_T(\phi)}{g'_T(\phi)} \tag{4.15}$$

where A is an undetermined constant. Let ϕ_1 be the solution to the boundary condition (4.9) at $x = 1$. Note that because of the presence of the boundary layer one cannot solve (4.9) directly in terms of zeros of K_T. In order to match the solution $\Phi_i(X)$ of the boundary layer equation (4.11) or (4.15) with that of the outer solution $\Phi_o(x)$ of equation (4.10), we must have

$$\Phi_i(X = 0) = \phi_1 \tag{4.16}$$

$$\lim_{X \to -\infty} \Phi_i(X) = \Phi_o(1) \tag{4.17}$$

If we imagine that equation (4.15) describes a dynamical system with X treated as the "time" variable then equation (4.17) implies that $\Phi_o(1)$ must be an unstable critical point with $A = 2f_T(\Phi_o(1))$ and $f'_T(\Phi_o(1)) < 0$. In order that equation (4.16) be satisfied, ϕ_1 must be in the α-limit set of the unstable equilibrium $\Phi_o(1)$. This requires that either $\phi_1 < \Phi_o(1)$ or $f_T(\phi_1) < f_T(\Phi_o(1))$. Similarly, a boundary layer at $x = 0$ must satisfy equation (4.15) with

$$\Phi_i(X = 1) = \phi_0 \tag{4.18}$$

$$\lim_{X \to \infty} \Phi_i(X) = \Phi_o(0) \tag{4.19}$$

where ϕ_0 is the solution to the boundary condition (4.8) at $x = 0$. It follows that $f'_T(\Phi_o(0)) > 0$ and either $\phi_0 > \Phi_o(0)$ or $f_T(\phi_0) < f_T(\Phi_o(0))$.

So far we have discussed criteria for carrying out the matching of inner and outer solutions of equations (4.7)-(4.9) successfully for fixed T without ascertaining whether or not a solution to the boundary value problem exists, and if it is unique. In order to proceed further, it is necessary to impose certain restrictions on the functions f_T and g_T. Suppose that there exists an open interval $J_T \subset \mathbb{R} \setminus \mathbb{Z}$ with $\phi_L, \phi_R \in J_T$ and such that the functions f_T and g_T satisfy the following hypotheses on J_T:

i) $f''_T \neq 0$ for all $\phi \in J_T$

ii) there exists $\phi_c \in J_T$ such that $f'_T(\phi_c) = 0$

iii) $|f'_T| < g'_T$ for all $\phi \in J_T$

For concreteness we shall take $f''_T > 0$ in hypothesis i); the analysis of the case $f''_T < 0$ is very similar. The following theorem then holds (see [34] for a proof).

Theorem 1. *Suppose that for a given T, $f''_T > 0$, ϕ_L, ϕ_R, ϕ_c exist in J_T, and $\phi_L \neq \phi_R \neq \phi_c$. Then there exists a unique formal solution to the boundary value problem (4.7)-(4.9) provided that the outer solution stays in the interval J_T.*

It can also be proven that if the continuum model has a formal solution (Theorem 1) then the original discrete model has an actual solution for sufficiently large N. Moreover, this solution converges (non-uniformly near boundary layers) to the solution of the continuum problem [34].

4.3. Finding a self-consistent T

The final step in our analysis is to take the collective period T to be a free variable. The qualitative features of the solution in Theorem 1 can change drastically as certain parameters of the model including T are varied. For example, the boundary layer can switch from the left to the right-hand side of the chain or there can emerge boundary layers on both sides. One thus finds that parameter space is divided into distinct regions and there are sharp transitions in the behaviour of the solution as the boundary separating parameter domains is crossed. The phase of the solution obtained depends on the relative positions of ϕ_L, ϕ_R, ϕ_c and whether or not the outer solution $\Phi_o(x)$ passes through the turning point ϕ_c.

Definition 1. *We shall say that a solution is of type I if its outer solution $\Phi_o(x)$ is bounded away from ϕ_c. It is of type II if there is an $\overline{x} \in (0,1)$ such that $\Phi_o(\overline{x}) = \phi_c$. A solution is of type III if either $\Phi_o(0) = \phi_c$ or $\Phi_o(1) = \phi_c$.*

We then have the following theorem, which is extracted from [34] where a detailed proof may be found.

Theorem 2. *Let*

$$\Omega(x,T) = I(x) + 2\epsilon f_T(\phi_c) \tag{4.20}$$

and take $\Omega_{\max}(T) = \max\{\Omega(0,T), \Omega(1,T), \Omega(x_c,T)\}$ where x_c is the point in $(0,1)$ where $\Omega(x,T)$ has its largest local maximum. Then the solution of Theorem 1 takes on one of six forms, and these cover all possibilities exactly once:

(a) Suppose that $\Omega_L(T) > \Omega_{\max}(T)$, $\phi_L < \phi_c$ and one of the following holds: (i) $\Omega_L(T) > \Omega_R(T)$ or (ii) $\Omega_L(T) < \Omega_R(T)$ and $\phi_R < \phi_c$. Then the solution is of type I with a boundary layer on the right and $\Omega(T) = \Omega_L(T)$

(b) Suppose that $\Omega_R(T) > \Omega_{\max}(T)$, $\phi_R > \phi_c$ and one of the following holds: (i) $\Omega_L(T) < \Omega_R(T)$ or (ii) $\Omega_L(T) > \Omega_R(T)$ and $\phi_L > \phi_c$. Then the solution is of type I with a boundary layer on the left and $\Omega(T) = \Omega_R(T)$

(c) Suppose that $\Omega(x_c,T) > \Omega_L(T), \Omega_R(T)$. Then the solution is of type II with boundary layers at both ends and $\Omega(T) = \Omega(x_c,T)$

(d) Suppose that $\Omega_L(T) > \max\{\Omega(x_c,T), \Omega(0,T)\} > \Omega_R(T)$ and $\phi_L > \phi_c$. Then the solution is of type II if $\Omega_{\max}(T) = \Omega(x_c,T)$ or of type III if $\Omega_{\max}(T) = \Omega(0,T)$. There are boundary layers at both ends and $\Omega(T) = \max\{\Omega(x_c,T), \Omega(0,T)\}$.

(e) Suppose that $\Omega_R(T) > \max\{\Omega(x_c,T), \Omega(1,T)\} > \Omega_L(T)$ and $\phi_R < \phi_c$. Then the solution is of type II if $\Omega_{\max}(T) = \Omega(x_c,T)$ or of type III if $\Omega_{\max}(T) = \Omega(1,T)$. There are boundary layers at both ends and $\Omega(T) = \max\{\Omega(x_c,T), \Omega(1,T)\}$.

(f) Suppose that $\Omega_R(T), \Omega_L(T) > \Omega_{\max}(T)$ *and* $\phi_R < \phi_c < \phi_L$. *Then the solution is of type II if* $\Omega_{\max}(T) = \Omega(x_c, T)$ *or of type III if* $\Omega_{\max}(T) \neq \Omega(x_c, T)$. *There are boundary layers at both ends and* $\Omega(T) = \Omega_{\max}(T)$.

Cases (a) and (b) of Theorem 2 typically occur when $I(x)$ is a monotone function and $\phi_L < \phi_c < \phi_R$. Case (c) occurs when there is a local region of the chain where $I(x)$ is sufficiently higher than the rest of the chain. Cases (d) and (e) occur when there is competition between anisotropy and a local gradient in external inputs (and hence frequencies). Case (f) is rather unusual and requires $f_T > 0$ for all $\phi \in J_T$ when $f_T'' > 0$.

Theorem 2 yields the piece-wise function $\Omega(T)$, which takes on one of six forms chosen from the set $\{\Omega_L(T), \Omega_R(T), \Omega(0,T), \Omega(1,T), \Omega(x_c,T)\}$ according to which of the six cases (a)-(f) holds for that particular value of T. Now suppose that the conditions of Theorem 1 hold for all $T \in \mathcal{I}$ where $\mathcal{I} \subset \mathbb{R}$ is some extended interval. We then determine a self-consistent collective period T for the phase-locked solution by solving equation (4.3) for the piece-wise function $\Omega(T)$.

4.4. Example: isotropic interactions, monotone input function

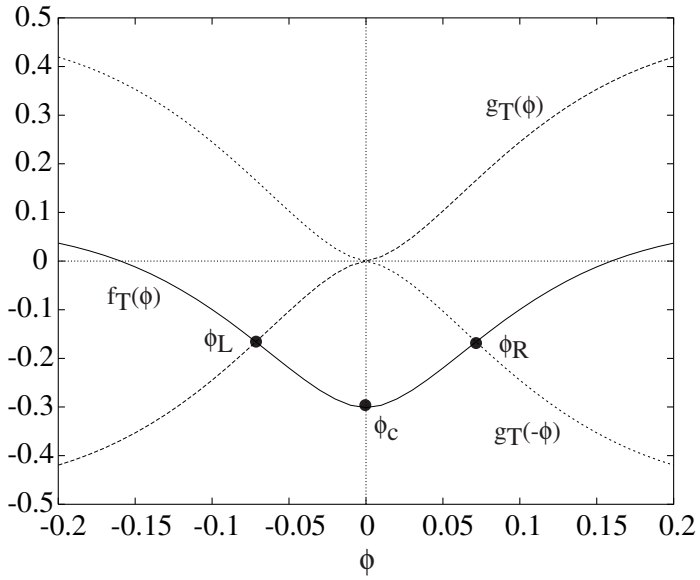


Figure 2: Even and odd functions $f_T(\phi), g_T(\phi)$ of an isotropic interaction function $K_T(\phi)$ defined by equations (3.13) and (3.15) for $\alpha = 10$, $\tau_d = 0.6$, and $T = 1.47$. $K_T(\phi)$ is related to the phase interaction function $H_T(\phi)$ of figure 1 according to equation (3.16).

As a simple example, suppose that $\phi_L < \phi_c < \phi_R$ for all $T \in \mathcal{I}$ and take $I(x)$ to be a monotone function of x with constant input gradient $\beta = dI/dx$.

Theorem 2 (cases (a) and (b)) implies that for a fixed T and a sufficiently small input gradient β there exists a unique solution for $\phi(x)$ with a single boundary layer whose location depends on the sign of the function $Qf_T^{''}$ where

$$Q = \Omega_L(T) - \Omega_R(T) = I(0) - I(1) + 2\epsilon\left[f_T(\phi_L) - f_T(\phi_R)\right] \tag{4.21}$$

For concreteness let $f_T^{''}(\phi) > 0$ for all $\phi \in J_T$. Then the boundary layer is on the right-hand side if $Q > 0$ and on the left-hand side if $Q < 0$. Suppose that we have an isotropic interaction function $K_T^+(\phi) = K_T^-(\phi) = K_T(\phi)$ with $K_T(\phi)$ given by equations (3.13) and (3.15). In figure 2 we plot the functions $f_T(\phi)$, $g_T(\phi)$ and the phases ϕ_L, ϕ_R, ϕ_c for $\alpha = 10$, $\tau_d = 0.6$, and $T = 1.47$. For these parameter values $K_T(\phi) = \chi H_T(\phi)$ (equation (3.16)) with $H_T(\phi)$ as in figure 1. Since f_T is even, $\phi_L = -\phi_R$, $\phi_c = 0$ and $f_T(\phi_L) = f_T(\phi_R)$ so that $Q = I(0) - I(1)$. Thus the position of the boundary layer is determined by the sign of the input gradient β. For a small negative gradient ($\beta < 0$), the outer solution satisfies $\Phi_o(x) \approx \phi_L < 0$. Recall that $\phi(x) \approx \phi(n/(N+1)) = \phi_n$ where ϕ_n is the phase difference between oscillators n and $n+1$ ($\phi_n = \theta_{n+1} - \theta_n$). Thus an outer solution satisfying $\Phi_o(x) < 0$ represents a travelling wave moving down the chain from lower numbered oscillators to higher numbered ones. A positive gradient, for which one has an outer solution $\Phi_o(x) \approx \phi_R > 0$, travels in the opposite direction. (In the absence of an input gradient, travelling waves can still be produced by having anisotropic interactions such that $f_T(\phi_L) \neq f_T(\phi_R)$. A detailed discussion of anisotropy will be given in section 5.1). Now suppose that we vary T over the interval $\mathcal{I}$. This alters the positions of ϕ_L and ϕ_R but ϕ_c remains fixed at zero. Thus, the system still satisfies the conditions of case (a) in Theorem 2 for $\beta < 0$ (or case (b) for $\beta > 0$) as T varies. Plotting $\Omega_L(T)$ as a function of T for $\beta < 0$ shows that $\Omega_L(T)$ has a unique intercept with $1/(1-\mathrm{e}^{-T})$ (see inset of figure 3), and this determines a unique, self-consistent travelling wave solution. In figure 3 we plot both the phase profile for a finite chain and that predicted by the corresponding continuum model. The corresponding case of a wave travelling up the chain is shown in figure 4.

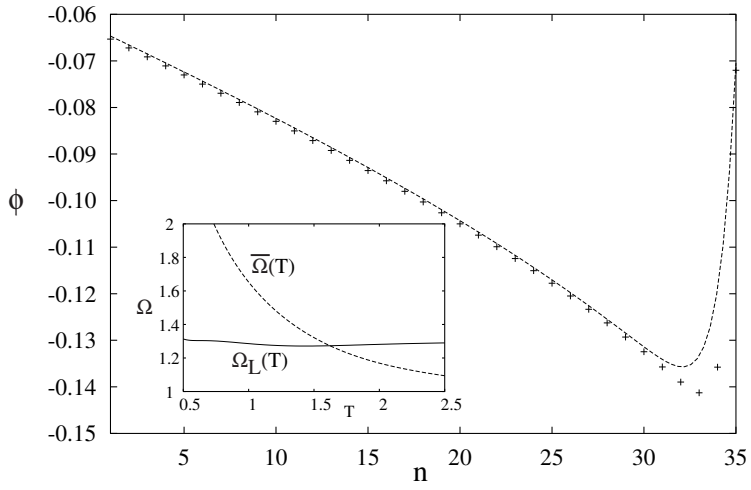


Figure 3: Type I solution determined by $\Omega_L(T)$ with $\phi_L < \phi_c$ and $\beta < 0$ yielding $\Omega_L(T) > \Omega_R(T)$. The interaction function is isotropic with the same parameter values as figure 2 (except for T, which is determined self-consistently). Also $I_1 = 1.3$, $\epsilon = 0.1$ and $\beta = -0.01\epsilon$. The points represent the solution for a chain with 36 integrate-and-fire oscillators, whilst the solid line is the solution of the ODE arising from the continuum approximation. Inset: Intersection of $\Omega_L(T)$ and $\overline{\Omega}(T) = [1 - \mathrm{e}^{-T}]^{-1}$ yields a unique value for the collective period, $T = 1.55$.

Remarks

(i) The numerical construction of travelling wave profiles for a finite chain of IF oscillators was obtained by the simultaneous solution of the set of algebraic equations defined in (4.1) for the relative phases $\phi_n = \theta_{n+1} - \theta_n$ and period T. Since this system of equations is analogous to the fixed point equations found in a phase-reduced model it is natural to consider the phases and period as fixed points of some dynamical system. In fact by allowing the phases and period to be time-dependent a numerical search for the travelliong wave profile reduces to finding the fixed points of a dynamical system. The XPP software package written by Bard Ermentrout is ideal for such purposes. (This is available from http://www2.pitt.edu/∼phase/). Although, of course, for large dimensional systems (as considered here) only initial data in the vicinity of the fixed point is likely to be of any practical use. We obtained such initial data by a direct simulation of a chain of IF oscillators. A simple fixed-step scheme for solving the IF dynamics gives an error proportional to the step-size when determining the firing times as threshold crossings. An improvement in accuracy was obtained by combining the fixed-step scheme with a simple linear interpolation for the estimate of the threshold crossing time. In this case it was reasonable for us to choose a 2nd order Runge-Kutta method for the fixed-step scheme with a step-size of 1×10^{-3}. Such a small step-size is necessary since firing times are in

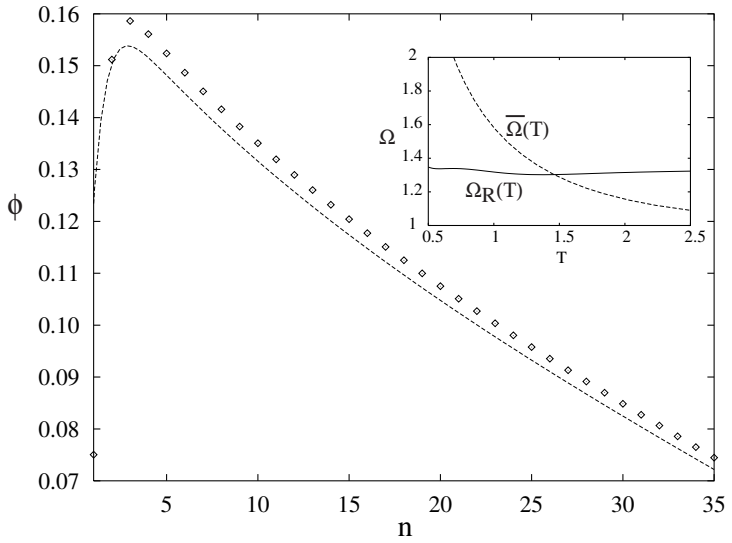


Figure 4: Type I solution determined by $\Omega_R(T)$ with $\phi_R > \phi_c$ and $\beta > 0$ yielding $\Omega_L(T) < \Omega_R(T)$. Same parameter values as figure 3 except $\beta = 0.01\epsilon$. Inset: Intersection of $\Omega_R(T)$ and $\overline{\Omega}(T) = [1 - \mathrm{e}^{-T}]^{-1}$ yields a unique value for the collective period, $T = 1.47$

part determined by previous spike train history and distortions in spike trains can spread rapidly through a network For biologically realistic choices of the function $\rho(t)$, firing events from the past only weakly influence those in the future. Consequently only the most recent 50 or so spikes were included in any spike train inputs to IF oscillators in the array. The combination of initial data from direct simulation of the IF system, with limited numerical precision, and a numerical solution of the equations that describe a phase-locked state proved sufficient in practice to construct travelling wave profiles for large chains of IF oscillators.

(i) The continuum equations describing a wave profile were solved by considering a discretization of space, such that the ODE model (4.7) could be approximated by a large set of coupled algebraic equations. For practical purposes 100 lattice points were used to approximate the continuum. This approximation generates a set of coupled equations reminiscent of the original lattice model, but with a modified coupling strength. The phases at the lattice points were obtained in an identical fashion to that described above. In this case, however, the period was chosen to satisfy $\Omega(T) = (1 - \mathrm{e}^{-T})^{-1}$ where $\Omega(T)$ was selected from the set $\{\Omega_L(T), \Omega_R(T), \Omega(0,T), \Omega(1,T), \Omega(x_c,T)\}$. Exploiting theorem 2 and knowledge from direct simulations of a large chain of IF oscillators, one can predict which one of these functions to chose. Once it has been chosen all one has to do is to check that the resultant wave profile is consistent with that obtained for a finite chain. It can be seen from figures 3 and 4 that the continuum approximation introduces only a small level of error. In particular, there

is good agreement between the self-consistent value of the period calculated for the finite chain ($T = 1.5486$) and the corresponding value constructed explicitly in terms of the boundary conditions for the continuum model ($T = 1.5484$). Note that the insets of figures 3 and 4 are slightly misleading, since they give the impression that $\Omega_L(T)$ and $\Omega_R(T)$ are approximately T-independent. In fact these functions show a significant variation with T outside the domain shown in the insets. There are two possible sources of error inherent in the continuum approximation. The first is that the ODE (4.7) depends upon the parameter $1/N$ although the discrete problem has no such explicit dependence upon N. The second is that the singular limit of the solutions to the ODE is not a good approximation to the solution of the continuum model with finite $1/N$. It is possible to establish numerically that the continuum model with $1/N$ finite is a reasonable approximation of the finite discrete model but is not well approximated by the singular limit $1/N \to 0$ used in the formal analysis.

(iii) The existence of a travelling wave solution as shown in figures 3 and 4 requires that the degree of detuning of the oscillators, which is determined by the size of the gradient β, be sufficiently small. This means in practice that $\beta = \mathcal{O}(\epsilon/N)$ (Kopell and Ermentrout 1986). For large detuning, one finds that one of the conditions necessary for Theorem 1 to hold breaks down, namely, the outer solution no longer lies within the interval J_T for $T \in \mathcal{I}$. This can lead to the formation of frequency plateaus along similar lines to phase models [11]; see section 5.3.

(iv) Our analysis of phase-locking in chains of integrate-and-fire oscillators is valid for arbitary values of the coupling ϵ, in contrast to the phase models considered by Kopell and Ermentrout [34]. Indeed, one finds that for fixed β, travelling wave solutions persist into the strong coupling regime since the effective level of detuning, β/ϵ, is reduced as ϵ increases. However, increasing ϵ can induce instabilities due to one or more eigenvalues of equation (3.20) crossing the unit circle leading to new forms of solution; see section 5.3. In the weak coupling regime, on the other hand, the stability of phase-locked solutions can be established by considering the corresponding phase model obtained by the averaging procedure of section 3.2. Note that it is possible for the phase model to be a reasonable approximation of the full IF model outside the weak coupling regime. However, there will exist some critical coupling beyond which it would be necessary to consider the full model.

(v) Theorems 1 and 2 require that the interaction function $H_T(\phi)$ is at least twice differentiable over the interval J_T. On the other hand, the interaction function $H_T(\phi)$ shown in figure 1 has a discontinuity in its first derivative at $\phi = \tau_d/T$. This does not cause a problem for the particular examples presented in this paper since this discontinuity lies outside the interval J_T.

5. Travelling wave instabilities

In this section we present a number of examples illustrating the effects of anisotropic interaction functions, non-monotonic inputs and strong coupling on the nature of travelling wave solutions.

5.1. Anisotropic interactions

One form of anisotropy occurs when the forward and backward couplings are unequal. To describe this form of anisotropy we introduce a parameter γ, $|\gamma| \leq 1$ such that

$$K_T^{\pm}(\phi) = (1 \mp \gamma) K_T(\phi) \tag{5.1}$$

where $K_T(\phi)$ is the isotropic interaction function. It is convenient to introduce the isotropic versions of the functions $f_T(\phi)$ and $g_T(\phi)$ as $\overline{f}_T(\phi)$ and $\overline{g}_T(\phi)$ such that (from equation (4.2))

$$f_T(\phi) = \overline{f}_T(\phi) - \gamma \overline{g}_T(\phi), \quad g_T(\phi) = \overline{g}_T(\phi) - \gamma \overline{f}_T(\phi) \tag{5.2}$$

Therefore, for an isotropic interaction

$$\overline{f}_T(\phi) = \frac{1}{2}[K_T(\phi) + K_T(-\phi)], \quad \overline{g}_T(\phi) = \frac{1}{2}[K_T(\phi) - K_T(-\phi)] \tag{5.3}$$

Hence, $\overline{f}_T(\phi)$ is an even function of ϕ whilst $\overline{g}_T(\phi)$ is an odd function of ϕ.

For $0 < \gamma \leq 1$ the forward coupling is stronger than the backward. The opposite is true for $-1 \leq \gamma < 0$, and when $\gamma = 0$ we have simply that $K_T^{\pm}(\phi) = K_T(\phi)$. Since ϕ_L and ϕ_R are defined via $K_T^-(-\phi_L) = 0 = K_T^+(\phi_R)$ the form of equation (5.1) shows that the anisotropy parameter γ does not play a direct role in their determination. The turning point ϕ_c is defined via the condition $f_T'(\phi_c) = 0$. If $\gamma = 0$, $f_T(\phi) = \overline{f}_T(\phi)$, which is even so $f_T'(0) = 0$ and hence $\phi_c = 0$. In general the turning point satisfies $\overline{f}_T'(\phi_c) = \gamma \overline{g}_T'(\phi_c)$ and depends upon $dK_T(\pm\phi)/d\phi = \pm T[P_T(\pm\phi) - K_T(\pm\phi)]$. For the completely anisotropic case $\gamma = 1$, we have $K_T^-(\phi) = 2K_T(\phi)$ and also $f_T(\phi) = \overline{f}_T(\phi) - \overline{g}_T(\phi) = K_T(-\phi)$. The equations for the forward-only coupled chain become

$$\Omega(T) = I_n + 2\epsilon K_T(-\phi_{n-1}), \quad n = 2, \ldots, N+1 \tag{5.4}$$

where $\Omega(T) = I_1$. We see from this equation and (4.10) (with $f_T(\phi) = K_T(-\phi)$) that the outer equation gives the exact phase difference showing that no boundary layers are present.

Assume for the moment that a self-consistent value of the period T can be found with $\phi_L < \phi_c < \phi_R$, $|\gamma| \leq 1$ and restrict attention to the case of a constant positive input gradient ($\beta > 0$). In the isotropic case ($\gamma = 0$), $\phi_L = -\phi_R$, $\phi_c = 0$ and $\Omega_L(T) < \Omega_R(T)$, which corresponds to case (b) of Theorem 2 with a boundary layer on the left-hand side and a wave travelling up the chain from right to left. Suppose that γ is now decreased so that ϕ_c tends towards ϕ_L and $f_T(\phi_L) > f_T(\phi_R)$. Recall that the position of the boundary layer depends on the sign of Qf_T'' with Q defined in equation (4.21). Q is dependent upon both the strength of anisotropy and the input gradient. Since $f_T'' > 0$, we find that Q becomes more positive as γ decreases. This does not change the position of the boundary layer and hence both the input gradient ($\beta > 0$) and the anisotropy ($\gamma < 0$) tend to make the waves travel up the medium in the direction of decreasing n. On the other hand, for positive γ the bias of the input gradient

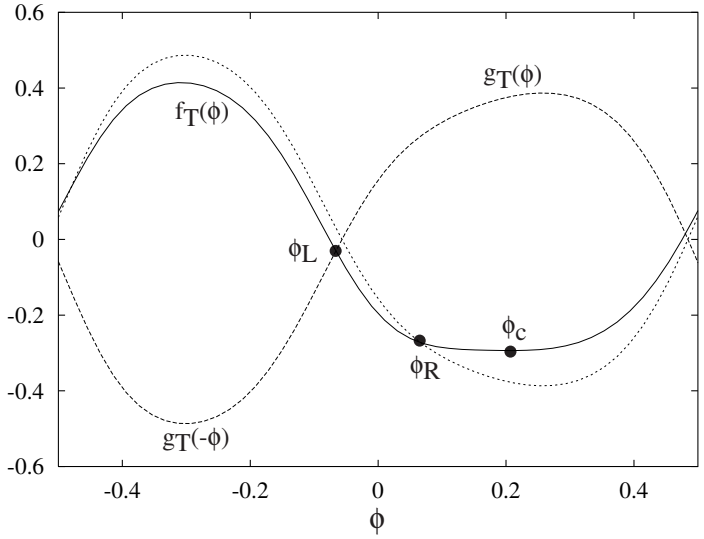


Figure 5: Functions $f_T(\phi), g_T(\phi)$ for an anisotropic interaction function $K_T^{\pm}(\phi) = (1 \mp \gamma)K_T(\phi)$ with $K_T(\phi)$ having the same parameter values as in figure 2 (except that $T = 1.48$), and $\gamma = 0.8$.

is opposite to that of the anisotropy. Hence, $Q = \Omega_L(T) - \Omega_R(T)$ is decreased and ϕ_c moves toward ϕ_R. If Q changes sign or ϕ_c crosses ϕ_R then (according to Theorem 2) the collective frequency is determined by $\Omega_L(T)$ and the waves will move *down* the medium. Such a travelling wave is shown in figure 6 for $\gamma = 0.8$ and the corresponding functions $f_T(\phi)$ and $g_T(\phi)$ are plotted in figure 5. Thus by altering the bias in the coupling that determines the position of the boundary layer a single network may support both forward and backward propagating waves.

From a more general perspective, one may regard $K_T^{\pm}(\phi)$ as arising from two independent ascending and descending synaptic pathways that determine the direction of wave propagation through their relative influences. In certain CPGs it is found that delays such as synaptic rise-times and transmission delays can differ along the two pathways, see for example [38] and references therein. This provides a second possible source of asymmetry for the interaction functions. (In the case of weakly-coupled oscillator chains, differences in timing between ascending and descending pathways may be incorporated by considering coupling functions that are phase-shifted versions of one another [34]). As an illustration, suppose that we introduce distinct delay parameters $\alpha^+ = 5, \alpha^- = 10$ and write $K_T^{\pm}(\phi) = K_T^{\pm}(\phi; \alpha^{\pm})$. The resulting functions $f_T(\phi)$ and $g_T(\phi)$ are shown in figure 7 where the asymmetry $f_T(\phi_L) \neq f_T(\phi_R)$ is clearly seen. In the case of zero input gradient, this anisotropy will produce a travelling wave down the chain since Q in equation (4.21) will be positive.

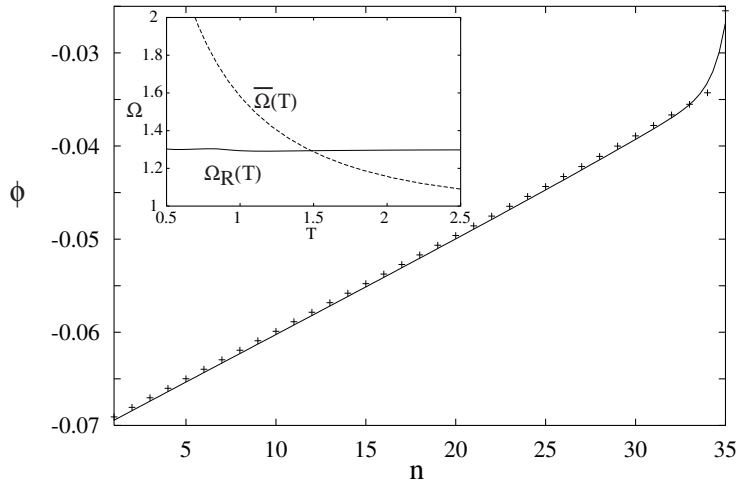


Figure 6: Type I solution determined by $\Omega_R(T)$ with $\phi_R < \phi_c$ and $\beta > 0$ yielding $\Omega_L(T) < \Omega_R(T)$. The interaction function is anisotropic with the same parameter values as figure 5. Also $I_1 = 1.3$, $\epsilon = 0.2$ and $\beta = 0.01\epsilon$. The points represent the solution for a chain with 36 integrate-and-fire oscillators, whilst the solid line is the solution of the ODE arising from the continuum approximation. Inset: Intersection of $\Omega_R(T)$ and $\overline{\Omega}(T) = [1 - \mathrm{e}^{-T}]^{-1}$ yields a unique value for the collective period, $T = 1.48$

5.2. Local regions of non-monotonic input

Assuming that the continuum limit approximation remains valid one may also explore the consequences of non-monotonic distributions for the input $I(x)$. In the uncoupled case, this would induce regions for which there is a local increase or decrease in the natural frequency. We write the input gradient as

$$I(x) = \widehat{I}(x) + \delta p(x) \tag{5.5}$$

where $\widehat{I}(x)$ is monotonically increasing in x, say, and $p(x)$ is nonzero only on a finite number of intervals on each of which it has a fixed sign. The parameter δ measures the strength of the local change in input, which we take in numerical experiments to be as shown in the inset of figure 8.

For the purposes of illustration, suppose that a solution belongs to class (b) of Theorem 2 with $\delta = 0$ and $f_T'' > 0$. If δ is increased but kept sufficiently small such that $\Omega_R(T) > \Omega_{\max}(T)$ then the solution remains of type I and is different from the $\delta = 0$ solution only on the support of $p(x)$. As δ increases $\Omega(x_c, T)$ grows until $\Omega(x_c, T) = \Omega_{\max}(T)$. Since $\Omega(x, T) = \widehat{I}(x) + \delta p(x) + 2\epsilon f_T(\phi_c)$ and $\widehat{I}(x)$ is increasing, $\Omega(x_c, T)$ can only exceed $\Omega_R(T)$ if δ is sufficiently large, ie

$$\delta > \delta^* \equiv [\widehat{I}(1) - \widehat{I}(x_c) + 2\epsilon f_T(\phi_R) - 2\epsilon f_T(\phi_c)]/[p(x_c) - p(1)] \tag{5.6}$$

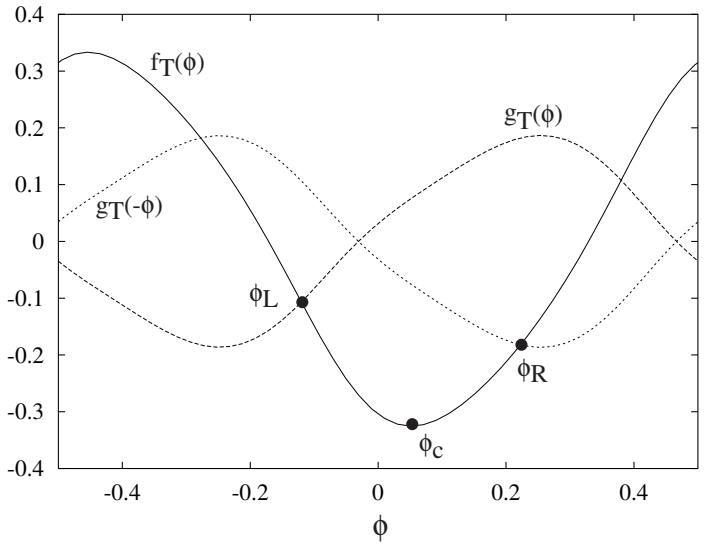


Figure 7: Functions $f_T(\phi), g_T(\phi)$ for an anisotropic interaction function $K_T^{\pm}(\phi;\alpha^{\pm})$ with $\alpha^+ = 5$, $\alpha^- = 10$, $T = 1.2$ and $\tau_d = 0.6$.

An example of this phenomenon is shown in figure 8. For $\delta < \delta^*$, the collective period T is determined by the self-consistent solution to the equation $[1 - \mathrm{e}^{-T}]^{-1} = \Omega_R(T)$, and hence T is constant since $\Omega_R(T)$ is independent of δ (see figure 8). On the other hand, above the threshold value δ^*, the solution is qualitatively different with boundary layers at both ends (type II) as illustrated in figure 9. The collective period is now determined by the self-consistent solution of the equation $[1 - \mathrm{e}^{-T}]^{-1} = \Omega(x_c, T)$ and thus varies with δ (see figure 8).

For sufficiently isotropic coupling (as used for the example of figure 3) $\phi = 0$ lies in the interval between $\Phi(0)$ and $\Phi(1)$ and the wave changes direction in the interior of this interval. In fact if $\phi_c = 0$ waves propagate outward from the support of $p(x)$. Hence if the local inputs are raised sufficiently in an interior part of the chain then a segment of the chain can *swim* backward. If the local change in input is too large, i.e. beyond point A in figure 8, then loss of frequency locking may occur due to the outer solution leaving the interval J_T (see figure 10). Interestingly, a local decrease in input does not cause a transition in solution type since if $\delta p(x) \leq 0$ for all x and $\Omega_{\max}(T) < \Omega_R(T)$ when $\delta = 0$ then $\Omega_{\max}(T) < \Omega_R(T)$ for all δ. Thus, there can be no solutions of type II in this case.

5.3. Instabilities in the weak and strong coupling regimes

Let us return to the example of isotropic interactions and a constant input gradient β (section 4.4). The parameter β determines the amount of detuning of

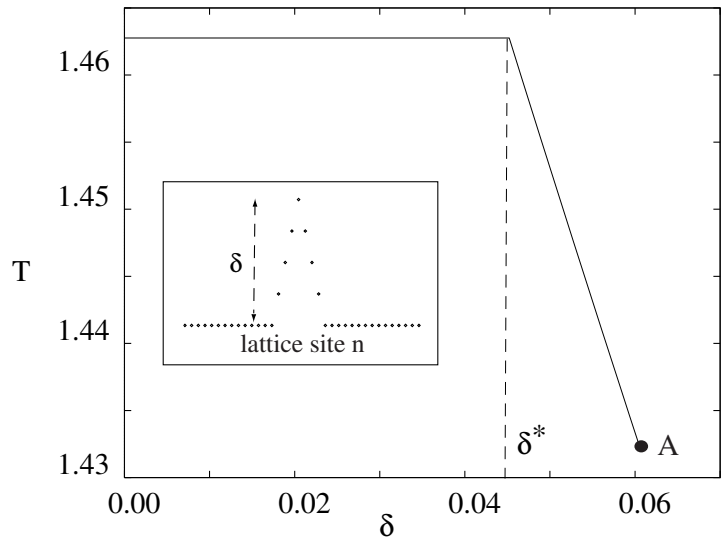


Figure 8: Self-consistent collective period T for a local perturbation of inputs of size δ and an isotropic interaction function with $\tau_d = 0.6$, $\alpha = 10$, $\epsilon = 0.1$ and $\beta = 0.01\epsilon$. Results shown are for a chain of 36 integrate-and-fire oscillators. For $\delta < \delta^*$ the collective frequency is determined by $\Omega_R(T)$. Beyond δ^* the collective frequency is detemined by $\Omega(x_c, T)$. At the point A phase-locking disappears. Inset shows shape of local perturbation of inputs across lattice.

the oscillator frequencies. In the weak coupling limit with $T \to \overline{T}$, phase-locked solutions will only depend on the parameters ϵ, β through their ratio β/ϵ. As previously found for weakly-coupled phase oscillators (Ermentrout and Kopell 1984), we would expect that increasing the level of detuning for fixed ϵ (small) leads to the disappearance of stable phase-locked solutions and the formation of frequency plateaus [48]. An example of strong detuning for moderate coupling is shown in figure 11, which was obtained by direct integration of equation (3.1). Outside the weak coupling regime, on the other hand, equation (3.14) cannot be solved for the phase differences ϕ_n independently of the collective period T. The latter is determined self-consistently to yield $T = T(\epsilon, \beta)$. Thus, phase-locked solutions now depend on both parameters ϵ, β independently. If ϵ is increased for fixed β it is possible for phase-locked solutions to persist into the strong coupling regime (see figure 12). However, increasing the coupling strength ϵ can induce instabilities due to one or more eigenvalues of equation (3.20) crossing the unit circle leading to new forms of solution (see inset of figure 12). In fact, large values of ϵ lead to a situation in which the bulk of the oscillators fire rapidly at twice the frequency of the boundary ones. In a system of neurons, however, the maximum firing rate is limited by the absolute refractory period to around 500Hz, although neurons in the cortex are observed to operate well below this level in the range $30 - 300$Hz. Since time has been measured in units

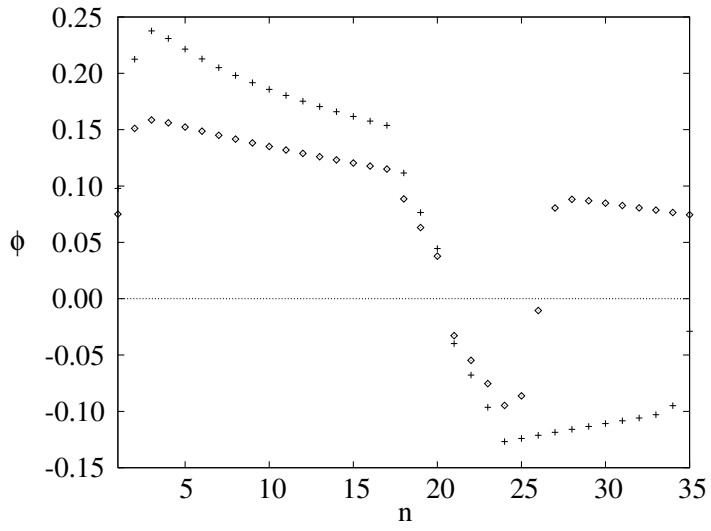


Figure 9: Type I Solution with $\phi_R > \phi_c$ determined by $\Omega_R(T)$ for a local increase in input at position 20 extending out to neighbours up to three units away is shown with $\diamond$'s and $\delta = \delta^* = 0.045$. The type II solution that occurs for a larger δ ($\delta = 0.05$) is shown with +'s. In this case the collective frequency is now determined by $\Omega(x_c, T) > \Omega_R(T)$. Results are for an isotropic interaction function with $I_1 = 1.3$, $\epsilon = 0.1$, $\tau_d = 0.6$, $\alpha = 10$ and $\beta = 0.01\epsilon$. Note that the transition region ($n \sim 20$) is not a layer satisfying the boundary layer equation but is a part of the outer solution.

of the decay constant of equation (3.1), for which we take 10ms as a realistic value, frequencies below 500Hz like those shown in the inset of figure 12, are biologically plausible.

Acknowledgments

This research was supported by grant number GR/K86220 from the EPSRC (UK). Much of the numerical analysis presented in the paper was performed with the aid of XPP developed by G. B. Ermentrout (Available from http://www2.pitt.edu/∼phase/)

References

[1] A T Winfree. *The Geometry of Biological Time.* Springer-Verlag, New York, 1980.

[2] L Glass and M C Mackey. *From Clocks to Chaos.* Princeton University Press, Princeton, 1988.

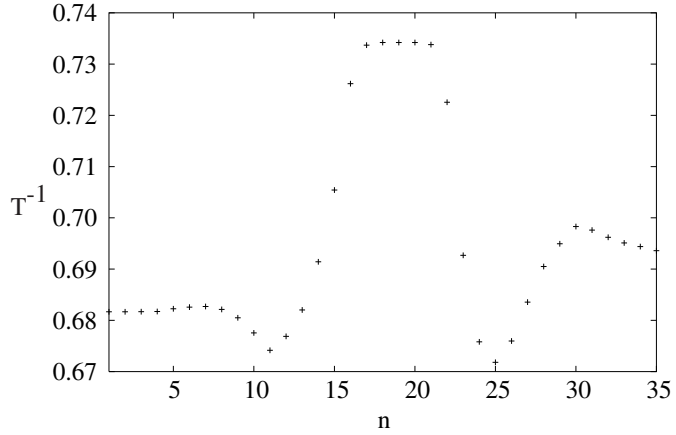


Figure 10: Distribution of frequencies T^{-1} across chain for a large local perturbation of inputs of size $\delta = 0.1$. All other relevant parameter values are as in figure 9.

[3] Y Kuramoto. *Chemical Oscillations, Waves and Turbulence*. Springer-Verlag, Berlin, 1984.

[4] P Hadley, M R Beasley, and K Wiesenfeld. Phase locking of Josephson-junction series arrays. *Phys. Rev. B.*, 38(13):8712–8719, 1988.

[5] K Y Tsang, R Mirollo, S H Strogatz, and K Wiesenfeld. Stability of incoherence in a population of coupled oscillators. *Physica D*, 48:103, 1991.

[6] H G Winful and S S Wang. Stability of phase locking in coupled semiconductor laser arrays. *Appl. Phys. Lett.*, 53:1894–1896, 1988.

[7] M Silber, L Fabiny, and L Wiesenfeld. Stability results for in-phase and splay-phase states of solid-state laser arrays. *J. Opt. Sci. America B.*, 10(6):1121–1129, 1993.

[8] N Fenichel. Persistence and smoothness of invariant manifolds for flows. *Indiana Univ. Math. J.*, 21:193–266, 1971.

[9] J Guckenheimer and P J Holmes. *Nonlinear Oscillations, Dynamical Systems and Bifurcations of Vector Fields*. Springer-Verlag, New York, 1983.

[10] R H Rand and P J Holmes. Bifurcation of periodic motions in two weakly coupled van der pol oscillators. *Int. J. Nonlinear Mech.*, 15:387–399, 1980.

[11] G B Ermentrout and N Kopell. Frequency plateaus in a chain of weakly coupled oscillators. *SIAM J. Math. Anal.*, 15:215–237, 1984.

[12] F C Hoppensteadt and I Izhekevich. *Weakly Connected Neural Nets*. Applied mathematical sciences;126. Springer-Verlag, New York, 1997.

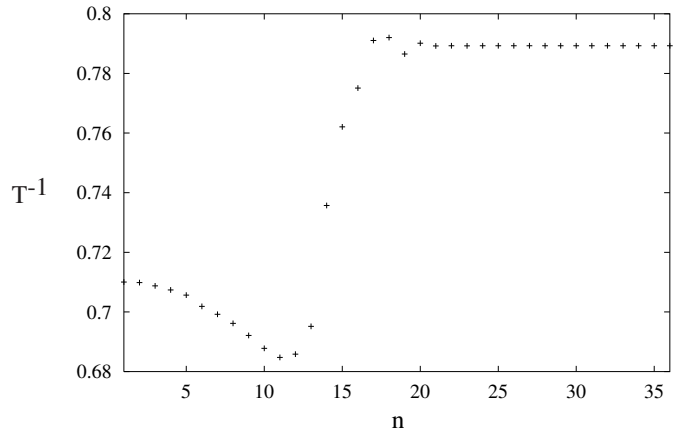


Figure 11: Plateau state in the case of strong detuning for a chain of 36 integrate-and-fire oscillators with isotropic coupling. Here $\alpha = 10$, $\tau_d = 0.6$, $I_1 = 0.3$, $\epsilon = 0.2$, and $\beta = 0.005$.

[13] J W Swift, S H Strogatz, and K Wiesenfeld. Averaging of globally coupled oscillators. *Physica D*, 55:239–250, 1992.

[14] S Watanabe and S H Strogatz. Constants of motion for superconducting Josephson arrays. *Physica D*, 74:197–253, 1994.

[15] A H Cohen, P J Holmes, and R H Rand. The nature of the coupling between segmental oscillators of the spinal lamprey generator. *J. Math. Biol.*, 13:345–369, 1982.

[16] N Kopell. Chains of coupled oscillators. In M A Arbib, editor, *The Handbook of Brain Theory and Neural Networks*, pages 178–183. MIT Press, 1995.

[17] H Sompolinsky, D Golomb, and D Kleinfeld. Cooperative dynamics in visual processing. *Phys. Rev. A*, 43:6990–7011, 1991.

[18] C M Gray and W Singer. Stimulus-specific neuronal oscillations in orientation columns of cat visual-cortex. *Proc. Natl. Acad. Sci.*, 86:1698–1702, 1989.

[19] M A Wilson and J M Bower. Cortical oscillations and temporal interactions in a computer simulation of piriform cortex. *J. Neurophysiol*, 67:981–995, 1992.

[20] A L Hodgkin and A F Huxley. A quantitative description of membrane current and its application to conduction and excitation in nerve. *J. Physiol. (London)*, 117:500–544, 1952.

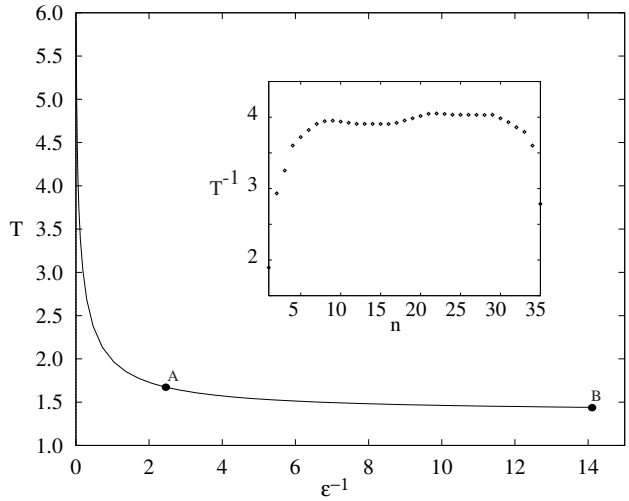


Figure 12: Numerical continuation, for $N = 35$, of a frequency locked solution into the strong coupling regime for an isotropic interaction function. Parameters are $\alpha = 10$, $\tau_d = 0.6$, $\beta = 0.001$ and $I_1 = 1.3$. Such solutions may destabilise if one or more of the eigenvalues of the linearised firing map (3.20) cross the unit circle. Numerical support for this possibility is provided in the inset where we show a stable non-frequency locked solution which exists at the point A ($\epsilon = 0.4$) in the strong coupling regime. At point B ($\epsilon = 0.07$), frequency locked states cease to exist in favour of multi-plateau states in which each group of oscillators has a differing frequency.

[21] D Hansel, G Mato, and C Meunier. Clustering and slow switching in globally coupled phase oscillators. *Phys. Rev. E.*, 48(5):3470–3477, 1993.

[22] H C Tuckwell. *Introduction to Theoretical Neurobiology*, volume I. Cambridge University Press, 1988.

[23] R E Mirollo and S H Strogatz. Synchronisation of pulse-coupled biological oscillators. *SIAM J. Appl. Maths*, 50(6):1645–1662, 1990.

[24] C Peskin. *Mathematical Aspects of Heart Physiology.* Courant Institute of Mathematical Sciences, New York University, New York, 1975.

[25] Y Kuramoto. Collective synchronisation of pulse-coupled oscillators and pulse-coupled excitable units. *Physica D*, 50:15–30, 1991.

[26] L F Abbott and C Van Vreeswijk. Asynchronous states in neural networks of pulse–coupled oscillators. *Phys. Rev. E.*, 48(2):1483–1490, 1993.

[27] A Treves. Mean-field analysis of neuronal spike dynamics. *Network*, 4:259–284, 1993.

[28] M Tsodyks, I Mitkov, and H Sompolinsky. Pattern of synchrony in inhomogeneous networks of oscillators with pulse interactions. *Phys. Rev. Lett.*, 71(8):1280–1283, 1993.

[29] W Gerstner. Time structure of the activity in neural-network models. *Phys. Rev. E*, 51(1):738–758, 1995.

[30] M Usher and M Stemmler. Dynamic pattern formation leads to $1/f$ noise in neural populations. *Phys. Rev. Lett.*, 74(2):326–329, 1995.

[31] S Bottani. Pulse-coupled relaxation oscillators: From biological synchronization to self-organized criticality. *Phys. Rev. Lett.*, 74(21):4189–4192, 1995.

[32] P C Bressloff, S Coombes, and B De Souza. Dynamics of a ring of pulse-coupled oscillators: a group theoretic approach. *Phys. Rev. Lett.*, 79:2791–2794, 1997.

[33] P C Bressloff and S Coombes. Symmetry and phase-locking in a ring of pulse-coupled oscillators with distriibuted delays. *Physica D*, 126:99–122, 1999.

[34] N Kopell and G B Ermentrout. Phase transitions and other phenomena in chains of coupled oscillators. *SIAM J. Appl. Math.*, 50:1014–1052, 1990.

[35] N Kopell and G B Ermentrout. Symmetry and phase-locking in chains of weakly coupled oscillators. *Comm. Pure Appl. Math.*, 39:623–660, 1986.

[36] J Connor. On exploring the basis for slow potential oscillations in the mammalian stomach and intestine. *Experiment. Biol.*, 81:153–173, 1979.

[37] W O Friesen and R A Pearce. Mechanisms of intersegmental coordination in leech locomotion. *Semin. Neurosci.*, 5:41–47, 1993.

[38] A Roberts. How does a nervous system produce behaviour? a case study in neurobiology. *Science Progress Oxford*, 74:31–51, 1990.

[39] G B Ermentrout and N Kopell. Oscillator death in systems of coupled neural oscillators. *SIAM J. Math. Anal.*, 50:125–146, 1990.

[40] G B Ermentrout and N Kopell. Multiple pulse interactions and averaging in systems of coupled neural oscillators. *J. Math. Biol.*, 29:195–217, 1991.

[41] L F Abbott and T B Kepler. Model neurons: From Hodgkin–Huxley to Hopfield. In L Garrido, editor, *Statistical Mechanics of Neural Networks*, pages 5–18. Springer–Verlag, 1990.

[42] G M Shepherd. Introduction to synaptic circuits. In G M Shepherd, editor, *The Synaptic Organization of the Brain*, pages 3–31. Oxford University Press, 1990.

[43] R Ritz, W Gerstner, and J L van Hemmen. Associative binding and segregation in a network of spiking neurons. In E Domany, J L van Hemmen, and K Schulten, editors, *Models of Neural Networks II*, pages 175–219. Springer-Verlag, 1994.

[44] C Van Vreeswijk, L F Abbott, and G B Ermentrout. When inhibition not excitation synchronizes neural firing. *J. Comp. Neurosci.*, 1:313–321, 1994.

[45] G B Ermentrout. N-M phase-locking of weakly coupled oscillators. *J. Math. Biol.*, 12:327–342, 1981.

[46] G B Ermentrout and N Kopell. Inhibition-produced patterning in chains of coupled nonlinear oscillators. *SIAM J. Appl. Math.*, 54(2):478–507, 1994.

[47] C Van Vreeswijk. Partial synchronization in populations of pulse-coupled oscillators. *Phys. Rev. E.*, 54(5):5522–5537, 1996.

[48] P C Bressloff and S Coombes. Travelling waves in a chain of pulse-coupled oscillators. *Phys. Rev. Lett.*, 80:4815–4818, 1998.